



# A Viscoelastic Model of Ice Stream Flow with Application to Stick-Slip Motion

Ryan T. Walker<sup>1,2\*</sup>, Byron R. Parizek<sup>3</sup>, Richard B. Alley<sup>4</sup> and Sophie M. J. Nowicki<sup>2</sup>

<sup>1</sup> Earth System Science Interdisciplinary Center, University of Maryland, College Park, MD, USA, <sup>2</sup> Cryospheric Sciences Laboratory, NASA Goddard Space Flight Center, Greenbelt, MD, USA, <sup>3</sup> Mathematics and Geoscience, Penn State DuBois, DuBois, PA, USA, <sup>4</sup> Department of Geosciences, Pennsylvania State University, University Park, PA, USA

Stick-slip motion such as that observed at Whillans Ice Stream, West Antarctica, is one example of transient forcing significantly affecting longer-term ice-stream dynamics. We develop and present a two-dimensional map-plane viscoelastic model of perturbations to ice-stream dynamics suitable for simulating and analyzing stick-slip behavior. Model results suggest important roles in stick-slip motion for both the elastic and viscous components of ice rheology, confirming and extending inferences drawn from simple models and observations. Elastic behavior depends on the rate of applied stress, at times allowing significant velocity perturbations with little change in accumulated stress perturbation; in contrast, viscous behavior depends on total accumulated stress and can lead to changes in ice-stream thickness over many stick-slip cycles.

**Keywords:** ice stream dynamics, stick-slip, viscoelasticity, ice rheology, Whillans ice stream, numerical ice sheet modeling

## OPEN ACCESS

### Edited by:

Alun Hubbard,  
University of Tromsø and Aberystwyth  
University, Norway

### Reviewed by:

Chris Borstad,  
The University Centre in Svalbard,  
Norway

Rachel Joanne Carr,  
Newcastle University, UK

Jake Walter,  
University of Texas at Austin, USA

### \*Correspondence:

Ryan T. Walker  
ryan.t.walker@nasa.gov

### Specialty section:

This article was submitted to  
Cryospheric Sciences,  
a section of the journal  
Frontiers in Earth Science

**Received:** 08 October 2015

**Accepted:** 07 January 2016

**Published:** 26 January 2016

### Citation:

Walker RT, Parizek BR, Alley RB and  
Nowicki SMJ (2016) A Viscoelastic  
Model of Ice Stream Flow with  
Application to Stick-Slip Motion.  
*Front. Earth Sci.* 4:2.  
doi: 10.3389/feart.2016.00002

## 1. INTRODUCTION

Fast-flowing ice streams are the primary outlets through which ice drains from interior regions of ice sheets into oceans (Bentley, 1987); it follows that understanding ice-stream dynamics is critical for projections of global sea level (e.g., Bindschadler et al., 2013). Streaming flow is typically enabled by some combination of a weak till bed and high subglacial water pressure, with the complexity of the processes involved leading to widely varying theories of basal sliding, from linear-viscous (Alley et al., 1987) to plastic (Tulaczyk, 2006) till rheology. Under these conditions, ice motion is primarily by basal processes, with vertical shear concentrated in the till and negligible in the ice, making the dynamics comparable to those of an ice shelf and permitting a depth-integrated modeling approach (MacAyeal, 1989). Ice streams are thus sensitive to perturbations in basal drag, and when longitudinal stresses are considered, to perturbations in hydrostatic pressure at the ice front.

Transient perturbations over shorter timescales (seconds to hours) require consideration of the elastic properties of ice in addition to the nonlinearly viscous flow that dominates ice stream dynamics over longer periods. For example, some ice streams (e.g., Bindschadler and Rutford) are known to be sensitive to transient forcings such as ocean tides (e.g., Anandakrishnan et al., 2003; Gudmundsson, 2007), and their behavior has been successfully analyzed with viscoelastic models (e.g., Gudmundsson, 2011; Walker et al., 2012). This modeling is of interest beyond study of the transients themselves, as matching model output with observations can lead to inference of physical properties (in this case, the form of the basal sliding law) that cannot be obtained from standard inverse methods applied to time-averaged velocity observations (e.g., Joughin et al., 2004).

In another example, Voytenko et al. (2015) apply the model of Walker et al. (2012) to observations of the velocity of the terminus of Helheim Glacier, Greenland by terrestrial radar interferometry to infer extremely weak ice in the floating portion.

One of the most complicated behaviors so far observed occurs on Whillans Ice Stream (WIS), which averages flow speeds over 300 m a<sup>-1</sup> in its lower reaches (the Whillans Ice Plain, WIP) despite moving only in short bursts roughly twice per day. Bindschadler et al. (2003) observed that this stick-slip behavior consists of long periods (6–18 h) of little motion, followed by bursts (10–30 min) of motion at over 30 times the average speed of WIS triggered by ocean tides under the Ross Ice Shelf. Subsequent studies have revealed a rich range of phenomena. A large, central “sticky spot” is especially important in supporting stress between motion events, then triggering motion events and generating far-field seismic energy (e.g., Wiens et al., 2008; Walter et al., 2011; Winberry et al., 2011; Pratt et al., 2014). In addition, one sticky spot near the grounding zone contributes to triggering of some motion events, and other sticky spots near the grounding zone provide localized resistance and generate additional seismic energy following initiation of fast motion (Walter et al., 2011, 2015; Winberry et al., 2011, 2014; Pratt et al., 2014).

Physical models for the stick-slip behavior are still under development. The sticky spots tend to occupy local maxima in subglacial hydrologic potential, and thus are better drained than surrounding regions, helping explain their locations (Alley, 1993; Horgan et al., 2013; Winberry et al., 2014). Geological heterogeneity may contribute (Walter et al., 2011; Muto et al., 2013). At least some of the sticky spots near the grounding zone may be related to till compaction resulting from the inland extension of ice-shelf tidal flexure; feedbacks with ice flow help generate hydropotential highs in the regions where downward flexure from rising tide favors till compaction (Christianson et al., 2013; Walker et al., 2013; Walter et al., 2015). The widespread occurrence of basal freeze-on beneath the ice streams of the Ross Embayment (e.g., Christoffersen et al., 2010), and the likelihood of regelation of stationary ice into subglacial sediments (Iverson, 1993), suggest that fault healing strengthens the sticky spots between motion events (Zoet et al., 2013; Winberry et al., 2014). However, Walter et al. (2015) suggested that the basic features of WIP stick-slip can be reproduced without spatial or temporal variations in bed strength. The value of a modeling framework to test hypotheses is clear.

In this study, we develop a two-dimensional viscoelastic model of transient perturbations to steady ice-stream flow and apply the model to an idealization of the WIP. Our primary goal is model development and demonstration rather than reproducing the full complexity of the observed motion of the WIP. We focus on the effects of sticky-spot formation and release on ice-stream dynamics, leaving the underlying mechanics of subglacial till for future work. Through a series of experiments, we demonstrate the importance of both elastic and viscous ice behavior for the dynamics of a single stick-slip cycle and longer-term ice thickness trends, respectively, confirming the inferences of Winberry et al. (2014) about interactions of viscous and elastic processes.

## 2. MODEL

The derivation of our model essentially follows that of Walker et al. (2012) except in two dimensions (map plane) rather than one (flowline). We begin with the MacAyeal-Morland equations (MacAyeal, 1989) for depth-integrated flow of ice streams and/or ice shelves:

$$\rho h \partial_t u + \partial_x (h(2\sigma_{xx} + \sigma_{yy})) + \partial_y (h\sigma_{xy}) = \rho g h \partial_x s + \tau_{bx}, \quad (1)$$

$$\rho h \partial_t v + \partial_y (h(2\sigma_{yy} + \sigma_{xx})) + \partial_x (h\sigma_{xy}) = \rho g h \partial_y s + \tau_{by}, \quad (2)$$

for ice surface elevation  $s$ , ice density  $\rho$ , and gravitational acceleration  $g$ . These equations assume all velocity arises below the ice (basal sliding or till deformation), so that the basal drag  $\tau_b$  becomes a horizontal body force and ice velocity does not vary with depth; however, they retain longitudinal stresses, allowing instantaneous ice velocity response to changes in applied stress from e.g., ice-shelf buttressing or basal “sticky spots.” Here, we have written the equations in terms of the deviatoric stresses  $\sigma_{ij}$  and have restored the inertial terms (using the velocity  $(u, v)$ ) that generally are negligible. Scaling arguments and experience with this model and the Walker et al. (2012) model show that these terms are indeed negligible even on tidal timescales, but our interest in stick-slip motion motivates their inclusion. The basal drag  $\tau_b$  depends on our choice of sliding law, and will be discussed further when the model is applied. (We note that our use of the “shelfy stream” force balance implicitly assumes that perturbations to  $\tau_b$  will be small enough not to produce significant internal deformation of the ice, which is a reasonable assumption for the experiments we will present). If we express the stresses and velocities as the sum of steady and perturbation components ( $\sigma = \bar{\sigma} + \tilde{\sigma}$ ,  $u = \bar{u} + \tilde{u}$ , etc.) and differentiate with respect to time, we obtain

$$\rho h \partial_{tt}^2 \tilde{u} + \partial_x (h(2\partial_t \tilde{\sigma}_{xx} + \partial_t \tilde{\sigma}_{yy})) + \partial_y (h \partial_t \tilde{\sigma}_{xy}) = \partial_t \tau_{bx}, \quad (3)$$

$$\rho h \partial_{tt}^2 \tilde{v} + \partial_y (h(2\partial_t \tilde{\sigma}_{yy} + \partial_t \tilde{\sigma}_{xx})) + \partial_x (h \partial_t \tilde{\sigma}_{xy}) = \partial_t \tau_{by}, \quad (4)$$

where the ice thickness  $h$  is taken as constant because we are interested in short timescales (seconds to hours).

In order to solve the perturbed Equations (3), (4), we must assume a rheology (flow law) for ice. The simplest viscoelastic rheology that displays both instantaneous elastic response and long-time viscous behavior is a Maxwell material. In one dimension, a Maxwell material can be conceptually modeled as an elastic spring and viscous dashpot in series, so that the same stress acts across both and the total strain is the sum of the strains in each element. For plane stress, the Maxwell rheology may be written in terms of the deviatoric stresses  $\sigma_{ij}$  as (e.g., Turcotte and Schubert, 2002)

$$\dot{\epsilon}_{xx} = \frac{1}{E} [\dot{\sigma}_{xx} + p - \nu(\dot{\sigma}_{yy} + 2p)] + \frac{1}{2\eta} \sigma_{xx}, \quad (5)$$

$$\dot{\epsilon}_{yy} = \frac{1}{E} [\dot{\sigma}_{yy} + p - \nu(\dot{\sigma}_{xx} + 2p)] + \frac{1}{2\eta} \sigma_{yy}, \quad (6)$$

$$\dot{\epsilon}_{xy} = \frac{1+\nu}{E} \dot{\sigma}_{xy} + \frac{1}{2\eta} \sigma_{xy}, \quad (7)$$

where  $\dot{\epsilon}_{ij}$  are the strain rates,  $E$  is Young's modulus,  $\eta$  is viscosity, and  $\nu$  is Poisson's ratio. We take  $\eta$  to be given by Glen's law and assume that it changes slowly enough to allow us to use the (possibly spatially varying) viscosity of the steady background state to calculate the perturbations. If we follow the usual practice and consider ice to be incompressible,  $\nu = 0.5$ , the pressure  $p$  is eliminated from the rheology (Cuffey and Paterson, 2010). We can then solve for the stress rate components:

$$\begin{aligned}\dot{\sigma}_{xx} &= \frac{2E}{3}(2\dot{\epsilon}_{xx} + \dot{\epsilon}_{yy}) - \frac{E}{3\eta}(2\sigma_{xx} + \sigma_{yy}) \\ &= \frac{2E}{3}(2\partial_x u + \partial_y v) - \frac{E}{3\eta}(2\sigma_{xx} + \sigma_{yy}),\end{aligned}\quad (8)$$

$$\begin{aligned}\dot{\sigma}_{yy} &= \frac{2E}{3}(2\dot{\epsilon}_{yy} + \dot{\epsilon}_{xx}) - \frac{E}{3\eta}(2\sigma_{yy} + \sigma_{xx}) \\ &= \frac{2E}{3}(2\partial_y v + \partial_x u) - \frac{E}{3\eta}(2\sigma_{yy} + \sigma_{xx}),\end{aligned}\quad (9)$$

$$\begin{aligned}\dot{\sigma}_{xy} &= \frac{2E}{3}\dot{\epsilon}_{xy} - \frac{E}{3\eta}\sigma_{xy} \\ &= \frac{E}{3}(\partial_y u + \partial_x v) - \frac{E}{3\eta}\sigma_{xy},\end{aligned}\quad (10)$$

where we have used the definitions of strain rates in terms of velocity components.

The final perturbed momentum equations are then found by substituting (8)–(10) into (3), (4) to obtain

$$\begin{aligned}\rho h \partial_{tt}^2 \tilde{u} + \partial_x \left[ \frac{Eh}{3\eta} (10\eta \partial_x \tilde{u} + 8\eta \partial_y \tilde{v} - 5\tilde{\sigma}_{xx} - 4\tilde{\sigma}_{yy}) \right] \\ + \partial_y \left[ \frac{Eh}{3\eta} (\eta \partial_y \tilde{u} + \eta \partial_x \tilde{v} - \tilde{\sigma}_{xy}) \right] &= \partial_t \tau_{bx},\end{aligned}\quad (11)$$

$$\begin{aligned}\rho h \partial_{tt}^2 \tilde{v} + \partial_x \left[ \frac{Eh}{3\eta} (\eta \partial_y \tilde{u} + \eta \partial_x \tilde{v} - \tilde{\sigma}_{xy}) \right] \\ + \partial_y \left[ \frac{Eh}{3\eta} (8\eta \partial_x \tilde{u} + 10\eta \partial_y \tilde{v} - 4\tilde{\sigma}_{xx} - 5\tilde{\sigma}_{yy}) \right] &= \partial_t \tau_{by},\end{aligned}\quad (12)$$

where advective terms resulting from the total time derivatives in (8)–(10) are negligible (cf. Reeh et al., 2003; Walker et al., 2012). Boundary conditions for these perturbed momentum equations may be essential (specified velocities) or natural [specified stress rates, using (3), (4) in the weak forms of (11), (12)]; for our rectangular domains, natural boundary conditions amount to zero longitudinal stress (rate) at transverse boundaries and zero shear stress (rate) at lateral boundaries. The system (8)–(12) is solved in MATLAB by fully implicit timestepping along with finite element spatial discretization using first-order triangular elements in the sparseFEM package (<https://bitbucket.org/maurow/sparsefem>).

### 3. APPLICATION

We use the model to investigate stick-slip behavior on an idealized domain similar to the Whillans Ice Plain. The domain

is an  $L \times L$  square, where  $L = 100$  km for most runs, with ice thickness varying linearly from  $h = 812.1$  m at  $x = 0$  to  $h = 803.4$  m at  $x = L$ . The background flow is taken to be in the positive  $x$  direction; we assume  $\bar{u} \sim 400$  m a<sup>-1</sup>, although this figure is used only for comparison with the perturbation velocity and does not enter the model. We impose a sticky spot at the center of the domain (analogous to the “central sticky spot” at “Ice Rise A” on WIP, Winberry et al., 2011) by setting, with  $x$  and  $L$  in m,

$$\tau_{bx} = \bar{\tau}_{bx} + F(t)\tau_b^{max} \exp \left[ -\frac{((x - L/2)^2 + (y - L/2)^2)/5000^2}{1} \right],\quad (13)$$

where  $0 \leq F(t) \leq 1$  describes the growth and decay of the sticky spot and  $\tau_b^{max} = 8$  kPa is its maximum strength. Note that the time-dependent part of  $\tau_{bx}$  averaged over a  $100 \times 100$  km domain with  $F(t) = 1$  is slightly more than 120 Pa, roughly comparable to the 300–350 Pa average pressure drop estimated by Winberry et al. (2009) for stick-slip events on WIP. For simplicity, we would like to assume that the bed outside of the sticky spot is perfectly plastic (consistent with Bindschadler et al., 2003), so that  $\partial_t \tau_{bx} = \partial_t \tau_{by} = 0$ . However, in practice it is necessary (see below) to assume a slight departure from perfect plasticity, which we linearize as  $\partial_t \tau_{bx} = \alpha^2 \tilde{u}$ ,  $\partial_t \tau_{by} = \alpha^2 \tilde{v}$ . Note that because this is a linearization of nearly plastic behavior,  $\alpha^2$  is much smaller than the usual coefficient  $\beta^2$  for a linear sliding law (of order  $10^4$ , vs. order  $10^8$ – $10^9$ ).

### 3.1. Reference Experiment

In our reference experiment, the sticky spot strengthens linearly over 12 h and then releases over 10 min (consistent with Bindschadler et al., 2003). More formally, we have

$$F(t) = \begin{cases} t/43200 & 0 \leq t \leq 43200 \\ (t - 43200)/600 & 43200 < t \leq 43800 \\ 0 & t > 43800 \end{cases}$$

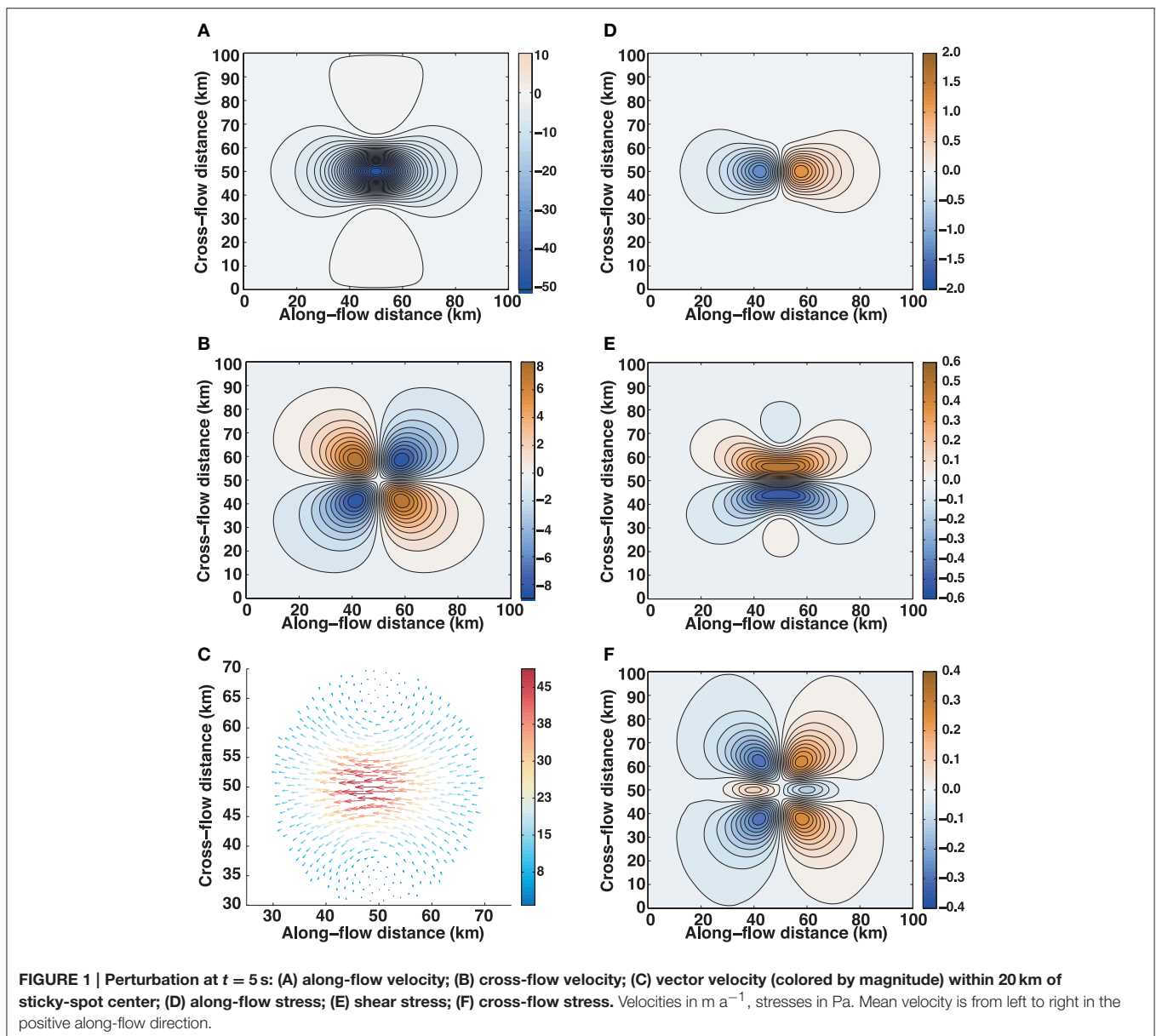
in (13). Note that this piecewise linear definition makes the rates of applied stress from the sticky spot constant (in time) for both the strengthening and weakening phases. [In practice, we smooth this function slightly by taking  $F'(43200) = 0$ .] We apply natural (zero perturbation stress rate) boundary conditions at the upstream and downstream boundaries, and essential (zero perturbation velocity) boundary conditions at the lateral boundaries. The basal drag coefficient is  $\alpha^2 = 4.3 \times 10^4$  Pa s m<sup>-1</sup>. With  $E = 3$  GPa and  $\eta = 10^{16}$  Pa s, the Maxwell relaxation time  $2\eta/E$  is roughly 77 days, so this experiment will be dominated by elastic behavior. The choice of  $E = 3$  GPa rather than the laboratory value of 9 GPa (Schulson and Duval, 2009) is consistent with past modeling studies of large bodies of damaged glacier ice (e.g., Anandakrishnan and Alley, 1997); the values of  $\eta$  in this study lie within the range of effective viscosities typically encountered in viscous (Glen's law) modeling of ice flow (Cuffey and Paterson, 2010).

The onset of sticking can be seen to begin directly over the sticky spot before spreading rapidly across the domain in roughly 3 min, reaching an essentially steady state within 10 min. Within 5 s of stick onset, ice over the sticky spot has already slowed by 48

$\text{m a}^{-1}$  relative to the background flow, despite stress perturbation components of only roughly 2 Pa or less (**Figure 1**). This is a consequence of elasticity, for which velocity depends only on the instantaneous rate of applied stress and not on the accumulated stress. Once the initial effects of inertia have been overcome, the velocity perturbation field remains the same throughout the strengthening phase due to the constant rate of applied basal stress, even as a considerable stress perturbation builds up. The along-mean-flow velocity perturbation reaches  $-382 \text{ m a}^{-1}$ , indicating that a sticky spot strengthening at this rate can essentially temporarily shut down the idealized ice stream. (This velocity perturbation is also comparable to the mean velocity of WIP). By the end of the strengthening phase, almost 20 kPa of along-mean-flow compressive stress and an equal amount of extensive stress have accumulated upstream and downstream,

respectively, of the sticky spot, as well as over 12 kPa of shear stress across the sticky spot (**Figure 2**).

The onset of slipping is essentially the same process in reverse, only with a much larger rate of applied stress because we assume failure of the sticky spot takes only 10 min following 12 h of strengthening. Slip begins directly over the weakening sticky spot and spreads rapidly; inertial effects are overcome and a steady velocity perturbation is reached after roughly 5 min. We note that the dependence of the elastic component of velocity on stress rate means that very high slipping velocities can be reached with release of only a fraction of the accumulated stress; the difference in, e.g.,  $\tau_{xx}$  between 5 s before and 5 s after slip onset is quite small, but the along-stream velocity perturbation is already over  $3 \text{ km a}^{-1}$  (**Figure 3**). Peak downstream velocities of  $\sim 74 \text{ m d}^{-1}$  are close to the roughly  $70 \text{ m d}^{-1}$  observed on



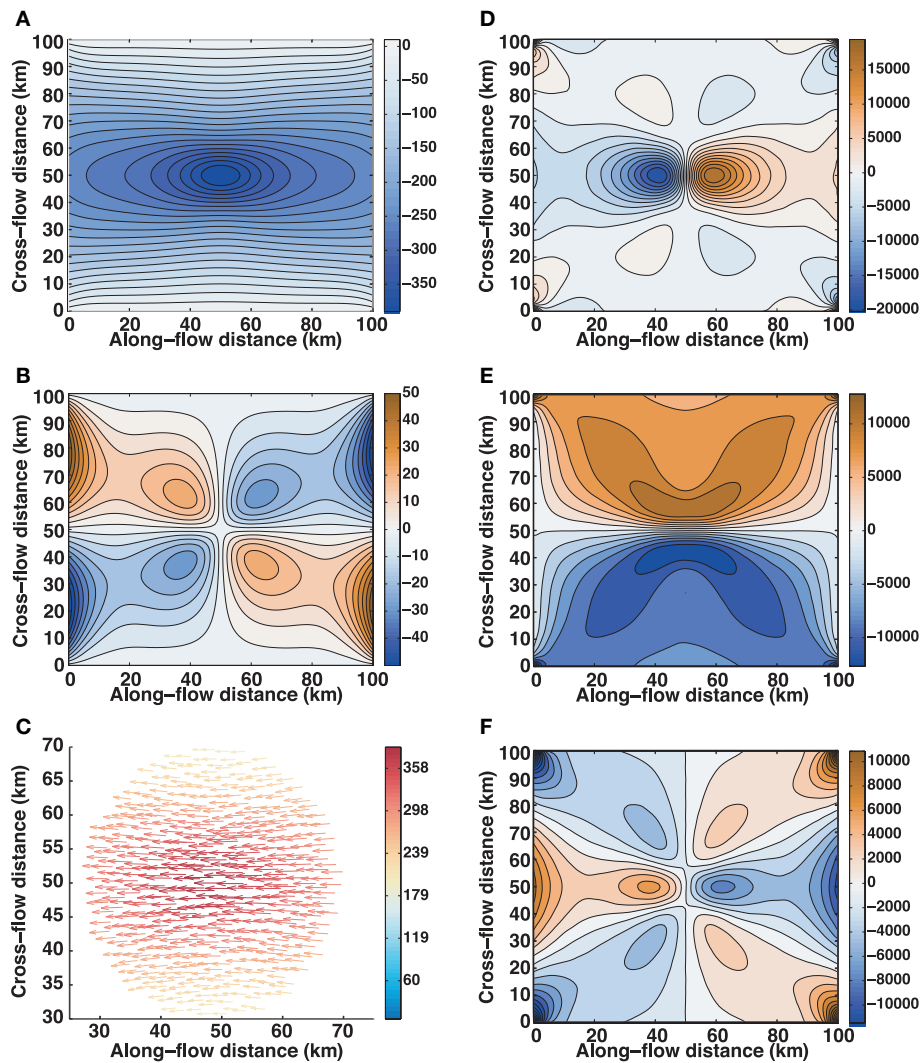


**FIGURE 2 |** Perturbation at  $t = 12$  h: (A) along-flow velocity; (B) cross-flow velocity; (C) vector velocity (colored by magnitude) within 20 km of sticky-spot center; (D) along-flow stress; (E) shear stress; (F) cross-flow stress. Velocities in  $\text{m a}^{-1}$ , stresses in Pa. Mean velocity is from left to right in the positive along-flow direction.

WIP for a slip event following a skipped slip (J. P. Winberry, pers. comm.), suggesting that this experiment is reasonable, but that the decrease in basal drag during a real WIP slip event is more gradual. By the end of slip (Figure 4), nearly all of the accumulated stress has been released (components  $\sim 1000$  Pa or less); due to inertial effects, the remaining stress takes roughly another 5 min to dissipate (components  $\sim 30$  Pa or less, and velocity components  $< 1 \text{ m a}^{-1}$ ).

### 3.2. Effects of Inertial Terms and Linearized Basal Drag

Having presented a typical experiment, we can now explain in greater detail the effects of the inertial and linearized basal drag terms. For clarity, we focus on the along-flow velocity perturbation  $\tilde{u}$  at the center of the sticky spot. If neither term is present, we have a perfectly plastic case in which the

effects of forcing propagate instantaneously across the domain; given our piecewise forcing (13),  $\tilde{u}$  is given by a step function (Figure 5), which is not realistic. If the inertial term is present without linearized basal drag, our model Equations (11), (12) allow fast wave solutions that cause a “ringing” effect in which the solution oscillates about a mean, potentially with relatively large amplitude. While these fast wave solutions are mathematically correct and would be reasonable for a seismic event, oscillations of this sort have not been observed on time scales of interest for ice-stream stick-slip events (Winberry et al., 2009, 2011). We therefore apply linearized basal drag both to represent a small departure from perfect plasticity and to damp out these fast waves, choosing the smallest  $\alpha^2$  that eliminates the oscillations. Because the basal drag term delays signal propagation (cf. Walker et al., 2014), the effect of adding the inertial term is rather small compared to the

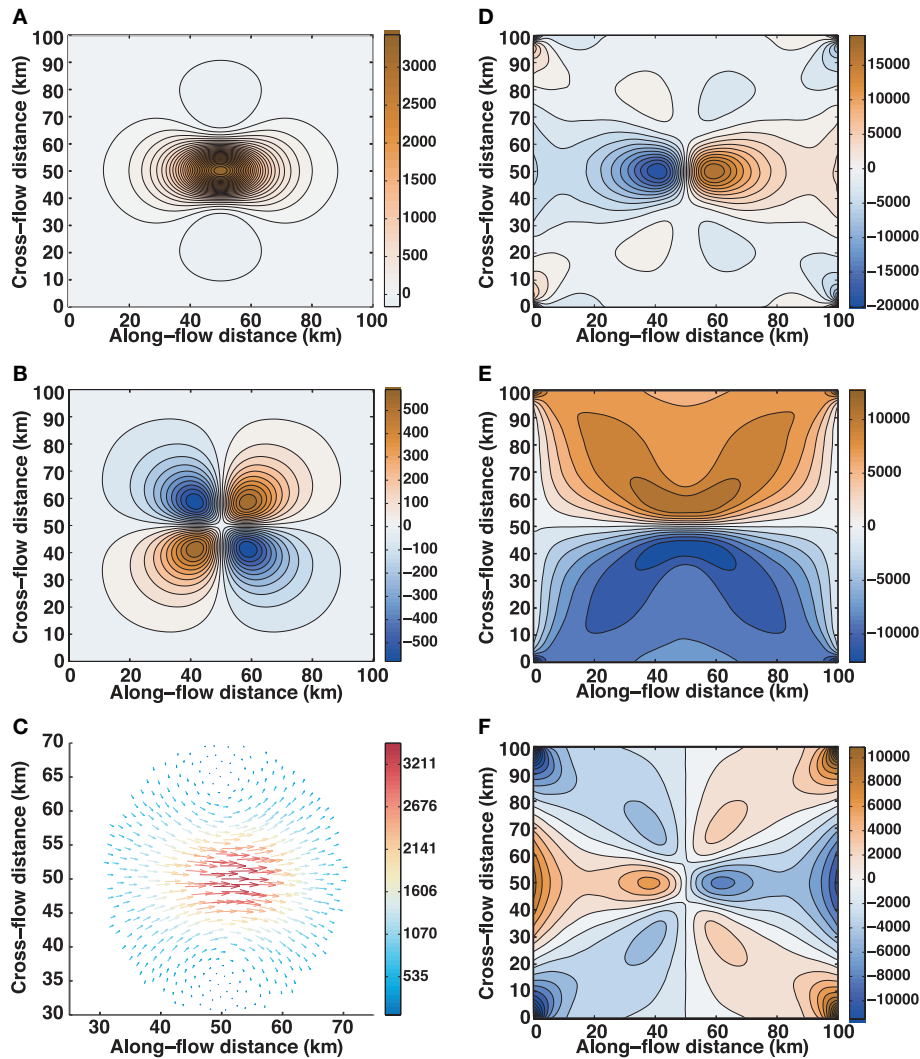


**FIGURE 3 |** Perturbation at  $t = 12\text{ h} + 5\text{ s}$ : (A) along-flow velocity; (B) cross-flow velocity; (C) vector velocity (colored by magnitude) within 20 km of sticky-spot center; (D) along-flow stress; (E) shear stress; (F) cross-flow stress. Velocities in  $\text{m a}^{-1}$ , stresses in Pa. Mean velocity is from left to right in the positive along-flow direction.

perfectly plastic case, resulting only in a small difference in timing.

### 3.3. Effects of Boundary Conditions

In order to examine the effects of the lateral boundary conditions, we expand the domain to  $L = 200\text{ km}$  and run with the same forcing. The first noticeable effect of the larger domain is that the linearized drag needed to damp fast waves is cut in half ( $\alpha^2 = 2.1 \times 10^4\text{ Pa s m}^{-1}$ ) due to the fast waves needing to travel twice as far before reflecting from the boundaries.

The onset of sticking is quite similar between the domains for roughly the first 30 s, before the perturbation has traveled far enough for shearing at the lateral boundaries to become significant. The time required for significant lateral shear to develop scales with the domain size, so that the time required for the disturbance to propagate across the domain and subsequently

reach an essentially steady state doubles. However, the influence of the lateral walls decreases with distance, as expected, so the along-mean-flow velocity perturbation is of greater magnitude ( $-453\text{ m a}^{-1}$ ) than for the original domain. During the slipping phase, the weakening of lateral shear becomes more readily apparent, as the along-mean-flow velocity perturbation reaches over  $32.6\text{ km a}^{-1}$ , though the relative increase in magnitude is 19% in both cases.

### 3.4. Effects of Viscosity

The previous experiments examined cases for which elastic behavior is dominant; we now consider truly viscoelastic cases in which viscous behavior is significant. In particular, we consider the situation discussed by Winberry et al. (2009) in which healing of the bed produces a concave down strength profile. We model this using

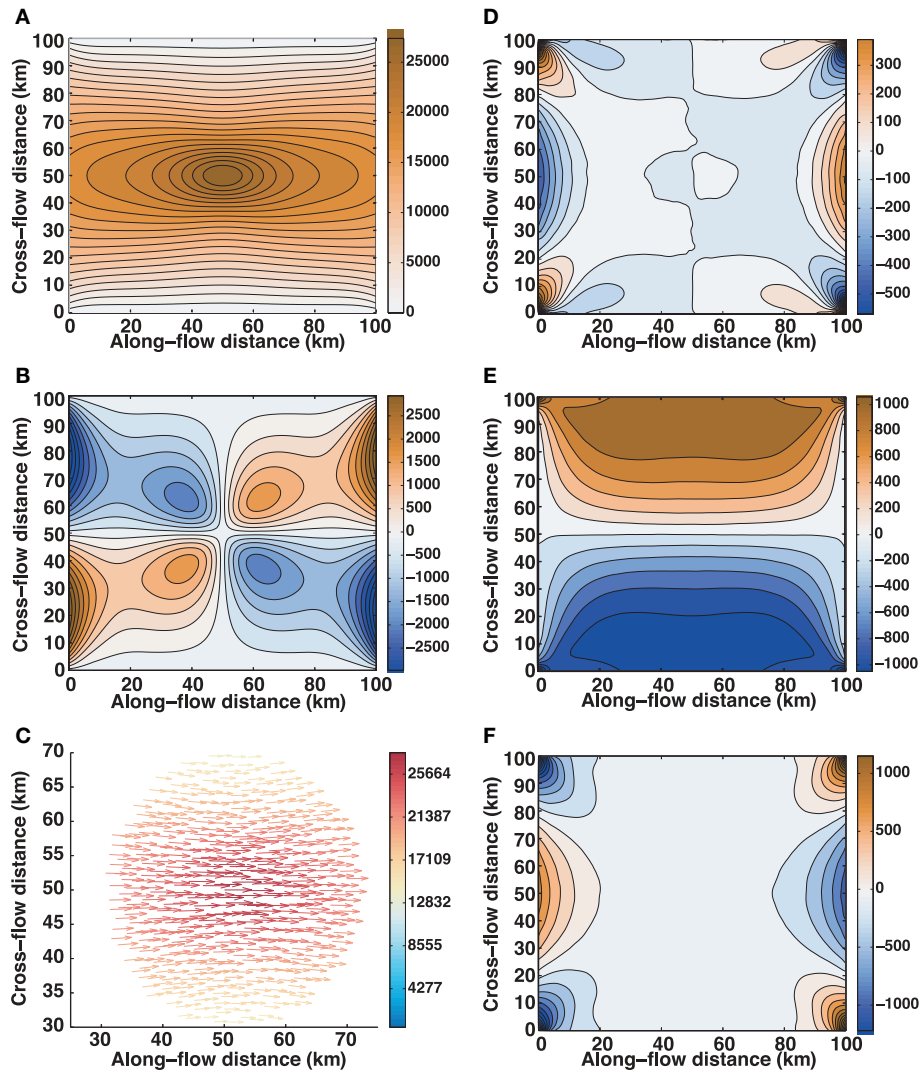


**FIGURE 4 |** Perturbation at  $t = 12\text{ h} + 10\text{ min}$ : (A) along-flow velocity; (B) cross-flow velocity; (C) vector velocity (colored by magnitude) within 20 km of sticky-spot center; (D) along-flow stress; (E) shear stress; (F) cross-flow stress. Velocities in  $\text{m a}^{-1}$ , stresses in Pa. Mean velocity is from left to right in the positive along-flow direction.

$$F(t) = \begin{cases} (t/43200)^{\frac{1}{n}} & 0 \leq t \leq 43200 \\ 1 - ((t - 43200)/600)^{\frac{1}{n}} & 43200 < t \leq 43800 \\ 0 & t > 43800 \end{cases}$$

in (13). In order to obtain reasonable elastic velocity perturbations, we use  $n = 1.5$  and weaken the sticky spot to  $\tau_b^{\text{max}} = 1.5\text{ kPa}$ . (Here, a reasonable perturbation is one in which the sticking phase slows, but does not reverse, the flow of the ice stream). We return to the  $L = 100\text{ km}$  domain for this experiment.

Based on the resulting profile of applied basal drag, we expect the elastic component of the perturbation (which depends on stress rate) to be largest at the onset of stick (or slip) and decrease thereafter, and the viscous component (which depends on accumulated stress) to increase over time. While the 10 min slip period is too brief for significant viscous effects to occur, the

12 h stick period allows this possibility. Using reasonable values of  $\eta$ , we can obtain behavior ranging from the purely elastic case to cases in which the viscous component dominates once the initially high stress rate diminishes after  $\sim 1\text{ h}$  (Figure 6). Interestingly, for  $\eta = 1 \times 10^{14}\text{ Pa s}$  (which gives a relaxation time of roughly 18 h) the increasing viscous component and decreasing elastic component offset to produce a very nearly steady along-flow velocity perturbation despite time-varying basal drag, a possibility suggested by Winberry et al. (2014).

Furthermore, the presence of a significant viscous component raises the possibility of stick-slip behavior affecting the long-term mean flow of the ice stream. For example, Winberry et al. (2014) observe a broad area thickening at  $\sim 0.3\text{ m a}^{-1}$  (from 2006–2010) upstream of WIP, which they attribute to viscous deformation between slips. Although our model assumes plane stress, the incompressibility condition

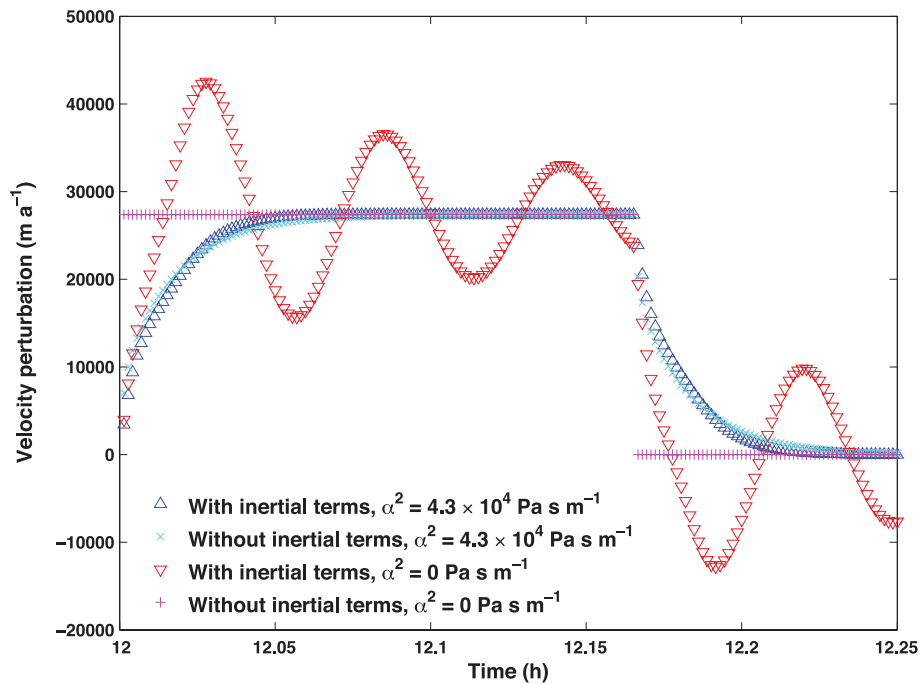


**FIGURE 5 |** Along-flow velocity perturbation at center of domain (over sticky spot), showing effect of including/excluding inertial terms and/or linearized basal drag.

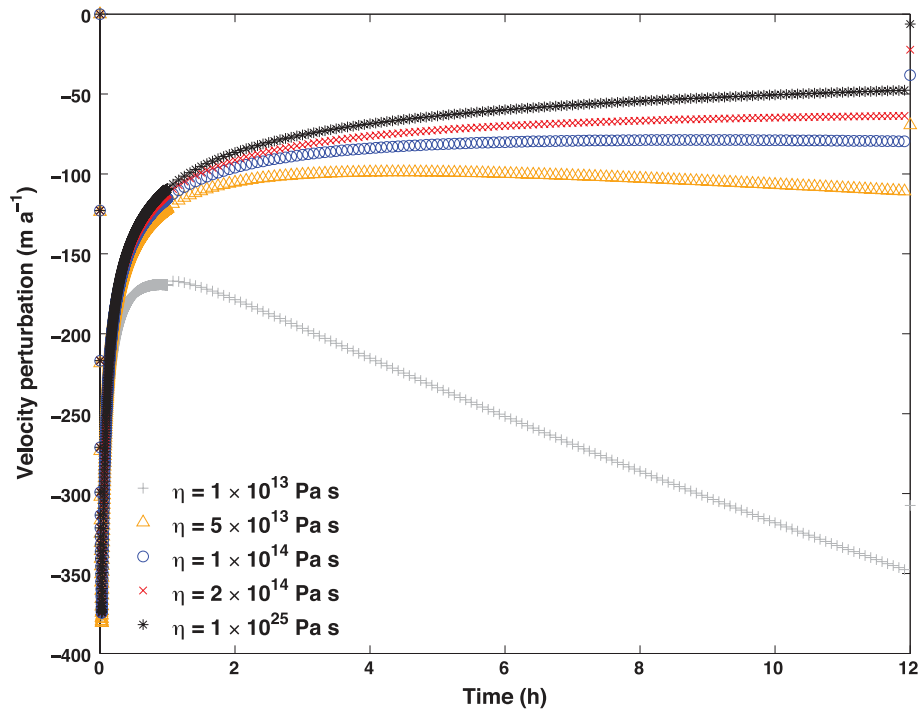


**FIGURE 6 |** Along-flow velocity perturbation at center of domain (over sticky spot), showing effect of varying viscosity. Results for  $\eta \geq 1 \times 10^{16}$  Pa s not shown due to overlap with the  $\eta = 1 \times 10^{25}$  Pa s experiment, which is an artificially high value chosen to obtain purely elastic behavior.

$$\partial_x \tilde{u} + \partial_y \tilde{v} + \partial_z \tilde{w} = 0 \quad (14)$$

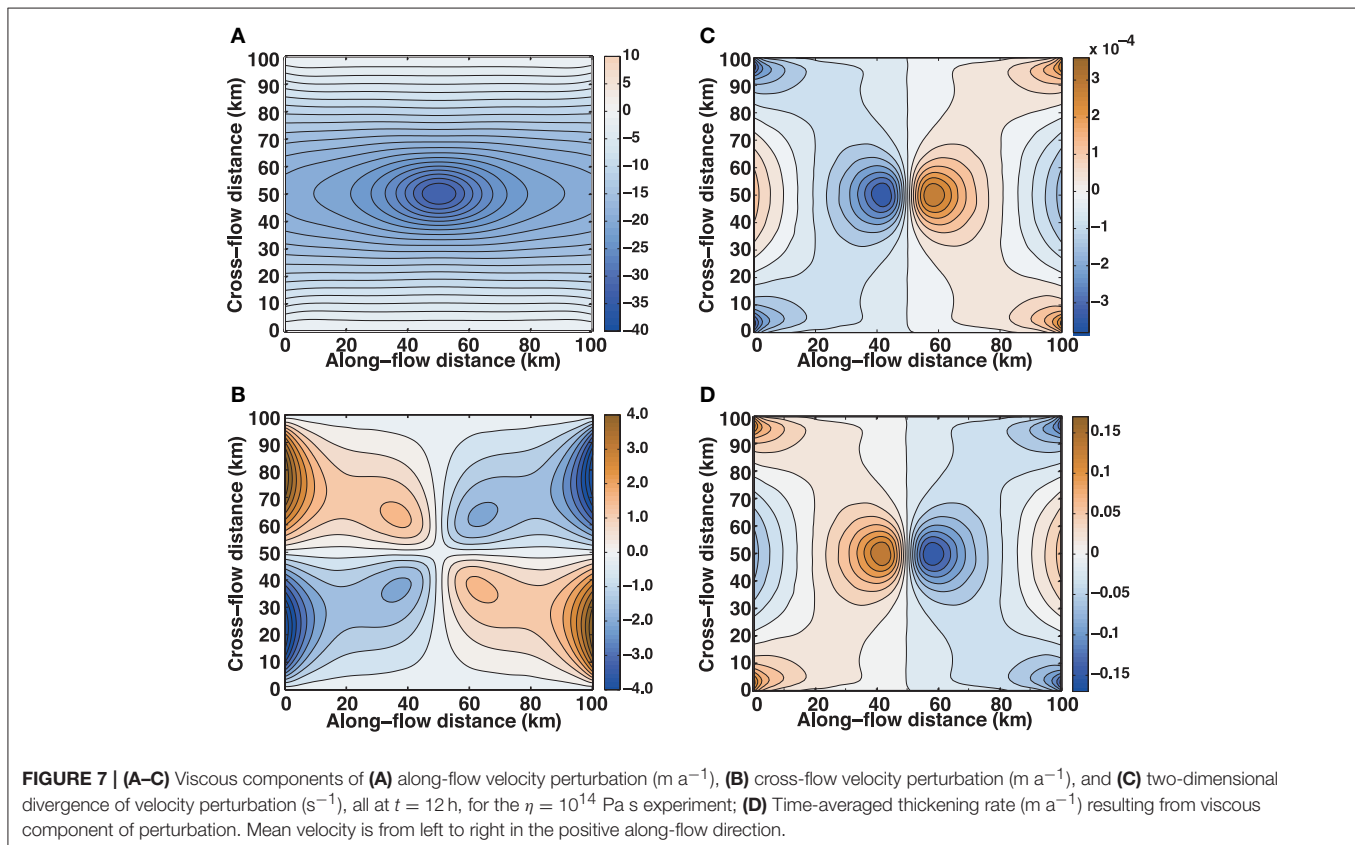
does imply a vertical velocity, and thus a thinning/thickening rate. The two-dimensional divergence  $\partial_x \tilde{u}_{visc} + \partial_y \tilde{v}_{visc}$  of the viscous component (for the  $\eta = 1 \times 10^{14}$  Pa s experiment) is easily calculated in the finite element framework provided by sparseFEM (Figure 7), and the vertical velocity found by integrating over depth. (Recall that for Maxwell rheology, the viscous component of a viscoelastic solution can be found by subtracting the elastic ( $\eta \rightarrow \infty$ ) solution). By averaging over a cycle, we see that, even though  $\tilde{w}$  is small enough to support our assumption that  $h$  is constant over shorter timescales, the thinning/thickening resulting from the viscous component of stick-slip (up to  $0.17 \text{ m a}^{-1}$ ) can be significant over years to decades. If we consider the case of a “skipped” slip (Winberry et al., 2014) and increase the period between slips to 24 h, we obtain the same pattern of  $dh/dt$  with magnitude increased roughly 70% (to a maximum of  $0.29 \text{ m a}^{-1}$ , close to the observed rate noted above). Further analysis will require a model with an advective component to determine the interaction of this thickening with the mean flow, and is a subject for future research.

## 4. DISCUSSION

We have long known that side drag is important in restraining well-lubricated ice streams (e.g., Raymond et al., 2001). This

new work confirms that such boundary effects are important for elastic as well as viscous flow, with important elastic differences when we increased the domain size beyond 100 km. The magnitude of velocity perturbations produced by a sticky spot of a given strength during both stick and slip phases increases with distance from fixed boundaries, i.e., zero-velocity essential boundary conditions. We experimented with natural as well as essential lateral boundary conditions; not surprisingly, we found some dependence of results on the nature as well as the location of the lateral boundary. (These experiments are not shown because “removing” a side wall from our reference experiment by changing to a natural boundary condition results in unrealistic velocity perturbations much larger than those resulting from doubling the domain size). We also note that the boundary conditions we have used, while reasonable in theory, have not been confirmed by observations. The results here thus suggest that additional physical and modeling work on the elastic coupling of ice streams to their surroundings would be valuable.

This study has focused on the effects of sticky-spot formation and release on ice dynamics by imposing idealized profiles of basal drag. However, real stick-slip events on WIP are paced by oscillations of the ocean tides, with ruptures propagating to trigger secondary slip events. The present model can be forced by ocean tides as a natural (stress) boundary condition, with velocity and stress perturbations propagating inland. In order to produce more realistic simulations in future work, the remaining challenge is to develop a model of bed strength consistent with



observations and to couple this with the existing ice-stream model. The current model thus provides a platform for further progress, as multiple bed models can be implemented and tested against observations.

Consistent with earlier studies (Winberry et al., 2014), the work here shows that viscous ice deformation in response to compression upglacier of the sticky spot and tension downglacier is not very important for WIS when it is slipping twice per day; however, over longer times, viscous deformation becomes notable. WIS is shifting toward one slip event per day (Winberry et al., 2014), with a pattern of skipped events that is influenced by the spring-neap tidal cycle, and other tidally influenced ice flow has been shown to respond to tidal components slower than diurnal (Gudmundsson, 2007). This interaction between viscous and elastic processes on ice streams means that viscoelastic ice-flow modeling offers advantages over models treating the different regimes separately.

## 5. SUMMARY

We develop and present a two-dimensional viscoelastic model of stick-slip ice-stream motion that is somewhat more complex than earlier slider block models (e.g., Winberry et al., 2009, 2014). In situations where elastic ice behavior is dominant, the velocity perturbation depends strongly on the rate of applied basal stress, so that very high velocities can be reached early in the slipping process, with the release of only a small fraction of the accumulated stress. We note that this is consistent with the conclusion of Winberry et al. (2009) that increases in slip magnitude are caused by increases in accumulated stress, provided that the duration of slip events remains roughly constant. In situations where viscous ice behavior becomes important, the viscous component of the perturbation grows with total accumulated stress; we show that this growth can offset decreases in the elastic component of ice velocity when the sticky-spot strength profile is concave down. Perhaps more importantly, we demonstrate that the

viscous components of repeated stick-slip cycles can gradually lead to thickening upstream and thinning downstream of the sticky spot. For parameters approximately representative of Whillans Ice Stream, the lateral boundaries affect stick-slip behavior even with an aspect ratio over 100:1, emphasizing the importance of characterizing these boundaries in field work and modeling. While work remains to be done regarding the mechanisms of sticky-spot growth and collapse, the model presented here does provide insight as to the importance of both components of viscoelastic ice rheology in stick-slip ice-stream dynamics.

## AUTHOR CONTRIBUTIONS

All authors contributed to the theory underlying this work. RW and BP were responsible for the mathematical development of the model. RW coded the numerical model and ran the experiments. RA proposed the experiments in Section 3.4. All authors participated in the writing of this manuscript and approved the final version.

## FUNDING

This research was supported by NASA under grants NNX12AD03A (RW), NNX12AP50G (RW) and NNX15AH84G (BP), and by the NSF under grants AGS 13-38832 (RA, BP), PLR 14-43190 (BP, RW), and PLR 04-24589 (RA, BP) to the Center for Remote Sensing of Ice Sheets (CREGIS). Additional funding was provided to SN by NASA through its Cryospheric Sciences and Modeling Analysis and Prediction Programs.

## ACKNOWLEDGMENTS

We thank Mauro Werder for sharing the sparseFEM MATLAB package, which he wrote with Christian Schoof and Ian Hewitt. We also thank the editor and reviewers for constructive comments that led to a greatly improved final manuscript.

## REFERENCES

- Alley, R. B., Blankenship, D. D., Bentley, C. R., and Rooney, S. T. (1987). Till beneath Ice Stream B: 3. Till deformation – evidence and implications. *J. Geophys. Res.* 92, 8921–8929. doi: 10.1029/JB092iB09p08921
- Alley, R. B. (1993). In search of ice-stream sticky spots. *J. Glaciol.* 39, 447–454.
- Anandakrishnan, S., and Alley, R. B. (1997). Tidal forcing of basal seismicity of ice stream C, West Antarctica, observed far inland. *J. Geophys. Res.* 102, 15183–15196. doi: 10.1029/97JB01073
- Anandakrishnan, S., Voigt, D. E., Alley, R. B., and King, M. A. (2003). Ice stream D flow speed is strongly modulated by the tide beneath the Ross Ice Shelf. *Geophys. Res. Lett.* 30, 1361. doi: 10.1029/2002GL016329
- Bentley, C. R. (1987). Antarctic ice streams – a review. *J. Geophys. Res.* 92, 8843–8858. doi: 10.1029/JB092iB09p08843
- Bindschadler, R. A., King, M. A., Alley, R. B., Anandakrishnan, S., and Padman, L. (2003). Tidally controlled stick-slip discharge of a west Antarctic ice stream. *Science* 301, 1087–1089. doi: 10.1126/science.1087231
- Bindschadler, R. A., Nowicki, S. M. J., Abe-Ouchi, A., Aschwanden, A., Choi, H., Fastook, J., et al. (2013). Ice-sheet model sensitivities to environmental forcing and their use in projecting future sea level (the SeaRISE project). *J. Glaciol.* 59, 195–224. doi: 10.3189/2013jog12j125
- Christianson, K., Parizek, B. R., Alley, R. B., Horgan, H. J., Jacobel, R. W., Anandakrishnan, S., et al. (2013). Ice sheet grounding zone stabilization due to till compaction. *Geophys. Res. Lett.* 40, 5406–5411. doi: 10.1002/2013GL057447
- Christoffersen, P., Tulaczyk, S., and Behar, A. (2010). Basal ice sequences in Antarctic ice stream: exposure of past hydrologic conditions and a principal mode of sediment transfer. *J. Geophys. Res. Earth Surf.* 115:F03034. doi: 10.1029/2009JF001430
- Cuffey, K., and Paterson, W. S. B. (2010). *The Physics of Glaciers, 4th Edn.* Boston, MA: Elsevier.
- Gudmundsson, G. H. (2007). Tides and the flow of Rutford Ice Stream, West Antarctica. *J. Geophys. Res.* 112:F04007. doi: 10.1029/2006JF000731
- Gudmundsson, G. H. (2011). Ice-stream response to ocean tides and the form of the basal sliding law. *Cryosphere* 5, 259–270. doi: 10.5194/tc-5-259-2011
- Horgan, H. J., Alley, R. B., Christianson, K., Jacobel, R. W., Anandakrishnan, S., Muto, A., et al. (2013). Estuaries beneath ice sheets. *Geology* 41, 1159–1162. doi: 10.1130/G34654.1

- Iverson, N. R. (1993). Regelation of ice through debris at glacier beds - implications for sediment transport. *Geology* 21, 559–562.
- Joughin, I., MacAyeal, D. R., and Tulaczyk, S. (2004). Basal shear stress of the Ross ice streams from control method inversions. *J. Geophys. Res.* 109:B09405. doi: 10.1029/2003JB002960
- MacAyeal, D. R. (1989). Large-scale ice flow over a viscous basal sediment: theory and application to Ice Stream B, Antarctica. *J. Geophys. Res.* 94, 4071–4087. doi: 10.1029/JB094iB04p04071
- Muto, A., Christianson, K., Horgan, H. J., Anandakrishnan, S., and Alley, R. B. (2013). Bathymetry and geological structures beneath the Ross Ice Shelf at the mouth of Whillans Ice Stream, West Antarctica, modeled from ground-based gravity measurements. *J. Geophys. Res. Solid Earth* 118, 4535–4546. doi: 10.1002/jgrb.50315
- Pratt, M. J., Winberry, J. P., Wiens, D. A., Anandakrishnan, S., and Alley, R. B. (2014). Seismic and geodetic evidence for grounding-line control of Whillans Ice Stream stick-slip events. *J. Geophys. Res.* 119, 333–348. doi: 10.1002/2013JF002842
- Ramond, C. F., Echelmeyer, K. A., Whillans, I. M., and Doake, C. S. M. (2001). “Ice stream shear margins,” in *The West Antarctic Ice Sheet: Behavior and Environment, Antarctic Research Series*, Vol. 77, eds R. B. Alley and R. A. Bindschadler (Washington, DC: American Geophysical Union), 137–155.
- Reeh, N., Christensen, E. L., Mayer, C., and Olesen, O. B. (2003). Tidal bending of glaciers: a linear viscoelastic approach. *Ann. Glaciol.* 37, 83–89. doi: 10.3189/172756403781815663
- Schulson, E. M., and Duval, P. (2009). *Creep and Fracture of Ice*. New York, NY: Cambridge University Press. doi: 10.1017/CBO9780511581397
- Tulaczyk, S. (2006). Scale independence of till rheology. *J. Glaciol.* 52, 377–380. doi: 10.3189/172756506781828601
- Turcotte, D. L., and Schubert, G. (2002). *Geodynamics, 2nd Edn*. New York, NY: Cambridge University Press. doi: 10.1017/CBO9780511807442
- Voytenko, D., Stern, A., Holland, D. M., Dixon, T. H., Christianson, K., and Walker, R. T. (2015). Tidally driven ice speed variation at Helheim Glacier, Greenland, observed with terrestrial radar interferometry. *J. Glaciol.* 61, 301–308. doi: 10.3189/2015JoG14J173
- Walker, R. T., Christianson, K., Parizek, B. R., Anandakrishnan, S., and Alley, R. B. (2012). A viscoelastic flowline model applied to tidal forcing of Bindschadler Ice Stream, West Antarctica. *Earth Planet. Sci. Lett.* 309, 128–132. doi: 10.1016/j.epsl.2011.12.019
- Walker, R. T., Parizek, B. R., Alley, R. B., Anandakrishnan, S., Riverman, K. L., and Christianson, K. (2013). Ice-shelf flexure and subglacial pressure variations. *Earth Planet. Sci. Lett.* 361, 422–428. doi: 10.1016/j.epsl.2012.11.008
- Walker, R. T., Parizek, B. R., Alley, R. B., Brunt, K. M., and Anandakrishnan, S. (2014). Ice-shelf flexure and tidal forcing of Bindschadler Ice Stream, West Antarctica. *Earth Planet. Sci. Lett.* 395, 184–193. doi: 10.1016/j.epsl.2014.03.049
- Walter, J. I., Brodsky, E. E., Tulaczyk, S., Schwartz, S. Y., and Pettersson, R. (2011). Transient slip events from near-field seismic and geodetic data on a glacier fault, Whillans Ice Plain, West Antarctica. *J. Geophys. Res.* 116:F01021. doi: 10.1029/2010JF001754
- Walter, J. I., Svetlizky, I., Fineberg, J., Brodsky, E. E., Tulaczyk, S., Barcheck, C. G., et al. (2015). Rupture speed dependence on initial stress profiles: insights from glacier and laboratory stick-slip. *Earth Planet. Sci. Lett.* 411, 112–120. doi: 10.1016/j.epsl.2014.11.025
- Wiens, D. A., Anandakrishnan, S., Winberry, J. P., and King, M. A. (2008). Simultaneous teleseismic and geodetic observations of the stick slip motion of an Antarctic ice stream. *Nature* 453, 770–774. doi: 10.1038/nature06990
- Winberry, J. P., Anandakrishnan, S., Alley, R. B., Bindschadler, R. A., and King, M. A. (2009). Basal mechanics of ice streams: insights from the stick-slip motion of Whillans Ice Stream, West Antarctica. *J. Geophys. Res.* 114:F01016. doi: 10.1029/2008JF001035
- Winberry, J. P., Anandakrishnan, S., Wiens, D. A., Alley, R. B., and Christianson, K. (2011). Dynamics of stick-slip motion, Whillans Ice Stream, Antarctica. *Earth Planet. Sci. Lett.* 305, 283–289. doi: 10.1016/j.epsl.2011.02.052
- Winberry, J. P., Anandakrishnan, S., Alley, R. B., Wiens, D. A., and Pratt, M. J. (2014). Tidal pacing, skipped slips and the slowdown of Whillans Ice Stream, Antarctica. *J. Glaciol.* 60, 283–289. doi: 10.3189/2014JoG14J038
- Zoet, L. K., Alley, R. B., Anandakrishnan, S., and Christianson, K. (2013). Accelerated subglacial erosion in response to stick-slip motion. *Geology* 41, 159–162. doi: 10.1130/G33624.1

**Conflict of Interest Statement:** The authors declare that the research was conducted in the absence of any commercial or financial relationships that could be construed as a potential conflict of interest.

Copyright © 2016 Walker, Parizek, Alley and Nowicki. This is an open-access article distributed under the terms of the Creative Commons Attribution License (CC BY). The use, distribution or reproduction in other forums is permitted, provided the original author(s) or licensor are credited and that the original publication in this journal is cited, in accordance with accepted academic practice. No use, distribution or reproduction is permitted which does not comply with these terms.